

The influence of real structure of gold catalysts in the partial hydrogenation of acrolein

C. Mohr,^a H. Hofmeister,^b and P. Claus^{a,*}

^a Department of Chemistry, Institute of Chemical Technology II, Darmstadt University of Technology, Petersenstr. 20, D-64287 Darmstadt, Germany

^b Max-Planck-Institute of Microstructure Physics, Weinberg 2, D-06120 Halle, Germany

Received 12 June 2002; revised 9 September 2002; accepted 10 September 2002

Abstract

The hydrogenation of acrolein on supported gold catalysts has been used as test reaction to study several aspects of structure sensitivity, i.e., the dependence of activity and selectivity on the size of gold particles. We focused our work on the influence of the geometrical configuration of the supported gold nanoparticles, namely the occurrence of multiply twinned particles (MTPs) and the degree of rounding. A higher number of MTPs resulted in a lowering of selectivity to the desired product, allyl alcohol, as well as a lowering of the turnover frequency. The higher amount frequency of a gold catalyst supported on TiO₂ compared to ZrO₂ is attributed to a higher degree of rounding of the former.

© 2003 Elsevier Science (USA). All rights reserved.

Keywords: Acrolein hydrogenation; Degree of rounding; Gold catalysts; MTPs; Structure sensitivity

1. Introduction

In recent years, gold has attracted growing interest in catalyst research since it has been shown, namely by Haruta and co-workers [1], that gold nanoparticles with sizes below 5 nm exhibit enhanced activity in CO oxidation already at room temperature, despite the inert character of gold. Therefore most work in this area is focused on oxidation reactions and only very few articles deal with hydrogenation on gold [2–9]. In earlier publications we described an unusual enhancement of the selectivity of supported silver catalysts for hydrogenation of α , β -unsaturated aldehydes into unsaturated alcohols [10], suggesting a subsequent investigation of the potential of supported gold particles for hydrogenation of the C=O group in the presence of an olefinic double bond. First results, showing much higher selectivities to the desired allyl alcohol in the hydrogenation of acrolein compared to conventional hydrogenation catalysts such as Pt/ZrO₂, were published recently by our group [11]. We also demonstrated

that the activity of such gold catalysts is enhanced by using suitable supports such as TiO₂ [12].

The issue of the catalytic reactivity of supported gold catalysts requires systematic study of possible influences such as support effects, bulk metal effects, support–particle interactions, gold particle size, and real structure (shape, degree of rounding).

To get more systematic knowledge of the influence of these different aspects, an experimental separation is desirable. For this purpose, a study of catalytic behavior on an inert support, varying only structural characteristics of the gold particles, is proposed. To this end, a measure of activity independent on metal loading and metal surface area is essential. This is realized by use of the turnover frequency (abbreviated as TOF), which is defined here as moles of acrolein converted per exposed gold surface site and second. When TOF and/or product selectivities vary with changing particle size, this reaction on that catalyst is termed structure-sensitive [13]. Under the supposition of an inert support, this is usually related to different adsorption behavior of reactants on surface sites of varying structural characteristics (faces, corners, edges, defects, etc., or an ensemble of more than one of such sites) of the catalytically active metal particle surface, the amount of which should change significantly with particle sizes in the

* Corresponding author.

E-mail address: claus@ct.chemie.tu-darmstadt.de (P. Claus).

URL address: http://www.ct.chemie.tu-darmstadt.de/ak_claus/index_de.html.

range of 1 to 10 nm [14]. TOF changes indicate structure sensitivity; however, selectivity changes do not, in general, since selectivity may further depend on the activity itself: Some products may occur only for higher TOF values. Nevertheless, the particle size dependence of selectivities in hydrogenation of α , β -unsaturated aldehydes is observed on a variety of supported metal catalysts [10,15,22,23].

In the following article, different strategies are applied to separate the different effects mentioned above. First, the reactivity of gold bulk metal is examined. This is followed by the issue of structure sensitivity of hydrogenation on supported gold catalysts. After that, the results of a more detailed study of the influence of specific structural properties of the gold on reactivity is presented. The influence of particle shape as well as the degree of rounding is of special interest.

2. Experimental

Gold powder was prepared by precipitation with hydroxylamine hydrochloride ($\text{NH}_2\text{OH} \cdot \text{HCl}$) as the reducing agent.

To ZrO_2 (Aldrich), gold was applied as $\text{Au}(\text{OH})_3$ through precipitation from tetrachloroauric acid (HAuCl_4 , ALFA) with NH_4OH . Various samples were prepared, differing just by precipitation at different pH values of the aqueous solution. The resulting samples are named Au/ ZrO_2 -DP22 (pH 5), Au/ ZrO_2 -DP23 (pH 6), and Au/ ZrO_2 -DP24 (pH 9). This precipitation step was followed by washing and filtering, drying of the precipitation product (393 K), calcination (3 h, 573 K, air, 5 h^{-1}), and reduction (573 K, H_2 , 5 h^{-1}). The standard reduction time was 3 h, variations from this treatment are indicated in the text. In these cases, the conditions of hydrogen treatment are included in the sample names.

The resulting catalyst samples were characterized by conventional transmission electron microscopy (CTEM) and high-resolution transmission electron microscopy (HRTEM). TEM was carried out on a JEM 1010 at 100 kV. Sizes and general morphology of the gold particles were investigated via a combination of bright-field and dark-field imaging to distinguish clearly between metal and support. Crystal structure of the gold particles, as well as support, was evaluated using HRTEM at a JEM 4010 (400 kV). For all TEM studies the sample powders were dispersed in isopropanol, agitated in an ultrasonic bath, and finally deposited on a commercial grade copper carrier grid (Grid 300, PLANO), which was coated with a carbon hole film. In the studies preference was given to the areas near the holes. Image analysis was performed using NIH image software [17].

The hydrogenation of acrolein (ALDRICH) was conducted in a computer-controlled fixed-bed micro reactor system, described earlier [18]. This apparatus makes it possible to carry out high-pressure gas phase hydrogenation of unsaturated organic compounds that are liquids with low va-

por pressure under standard conditions. The following test conditions were applied: temperature 513 K, total pressure $p_{\text{total}} = 2 \text{ MPa}$, molar ratio hydrogen/acrolein $\gamma = 20$, and reciprocal space time $W/F_{\text{Ac},0} = 15.3 \text{ g h mol}^{-1}$, with W as the weight of catalyst and F the molar flow of acrolein. Deviations from these standard conditions are given in the text. The reproducibility of the catalytic measurements is $\pm 2\%$ (with respect to the absolute value of conversion and selectivity).

In principle, the resulting products of acrolein (AC) hydrogenation may be propionaldehyde (PA, by hydrogenation of the C=C group and/or isomerization of allyl alcohol) and allyl alcohol (AyOH, by hydrogenation of the C=O group) and furthermore *n*-propanol (*n*-PrOH) as a result of the subsequent reaction of allyl alcohol and/or propionaldehyde and C_2 and C_3 hydrocarbons (HC, through decarbonylation, dehydration).

The reactor effluents were analyzed on line with a HP 5890 gas chromatograph, equipped with a flame ionization detector and a 30 m J&W DB-WAX capillary column.

Since the conversions measured on some catalysts were in some cases relatively low, a certain conversion even without catalyst had to be considered, even though the latter was very low (in general below 0.5% at 573 K).

The TOF was calculated from $\text{TOF} = r_{\text{Ac}}/n_{\text{OF}}$. There-with, r_{Ac} is the total amount of acrolein converted per weight of gold per second, and n_{OF} the amount of gold at the surface. The latter is calculated from $n_{\text{OF}} = n_{\text{total}} * D$, where n_{total} is the total amount of gold and D the degree of dispersion (i.e., the surface-to-volume ratio), estimated by TEM.

The specific surface area and pore structure of the resulting catalytic systems were further characterised by nitrogen physisorption on a Sorptomatic 1990 (Fisons), except for the gold powder, which was surveyed in a Micromeritics Gemini III.

3. Results and discussion

3.1. Structure sensitivity

3.1.1. Reactivity of gold powder and support

High activities in CO oxidation on gold/support catalysts are particularly attributed to the participation of the gold-support interface or to quantum size effects [1]. Investigation of the performance of unsupported gold powder makes it possible to separate such influences from the contribution of bulk-like gold itself. Thus, the origin of our previous findings of relatively high activities and selectivities to allyl alcohol in the hydrogenation of acrolein may be explained on that basis.

For the unsupported gold powder, a relatively high activity was measured; however, the main product was propionaldehyde with low selectivities to allyl alcohol (7%, Table 1). To enable estimation of turnover frequency (TOF), nitrogen physisorption was applied. The resulting BET

Table 1

Catalytic properties of different supported gold catalysts in the hydrogenation of acrolein (at standard conditions: $T = 513$ K, $p_{\text{total}} = 2$ MPa, molar ratio $\text{H}_2/\text{Ac} = 20$, $W/F_{\text{Ac},0} = 15.3$ g h mol⁻¹)

Catalyst	X_{Ac} [%]	r_{Ac} [$\mu\text{mol}(\text{g}_{\text{Au}} \text{s})^{-1}$]	Selectivities [%]				d_{Au} [nm]	D	TOF [s ⁻¹]
			AyOH	PA	<i>n</i> -PrOH	HC			
Gold powder	12 ^a	0.11 ^a	7	93	0	0	9500	1.8×10^{-4}	0.116
Au/ZrO ₂ -DP22 R573	5	49	35	70	1	0	7.7 ± 0.3	0.20	0.045
Au/ZrO ₂ -DP22 R573 18h	3	22	20	80	0	0	9.2 ± 12.4	0.17	0.022
Au/ZrO ₂ -DP22 R723	5	44	37	63	0	1	8.3 ± 9.9	0.19	0.045
Au/ZrO ₂ -DP23 R573	18	203	30	60	8	2	6.9 ± 9.1	0.22	0.182
Au/ZrO ₂ -DP24 R573	39	379	15	57	21	8	4.0 ± 3.9	0.35	0.213
	5 ^b	88 ^b	28	66	4	2			0.120

The specific rate related to the gold content is termed as r_{Ac} . Turnover frequencies (TOF) are calculated from dispersions D derived from TEM mean particle sizes.

^a $W/F_{\text{Ac},0} = 66.3$ g h mol⁻¹.

^b $W/F_{\text{Ac},0} = 6.8$ g h mol⁻¹.

surface (0.033 ± 0.0005) m² g⁻¹ of the gold powder was equated with the active surface. Moreover one could apply the established equations to derive a formal mean particle size from the active surface [19], followed by calculating the degree of dispersion with an onion-like shell model [20].

It is now clear that bulk gold can already act as a (noninert!) catalyst, working however at enhanced temperatures. Thermal activation seems likely, as has been more extensively discussed by Bond and Thompson [21]. It becomes clear that the potential of gold for hydrogenation cannot be explained exclusively by quantum size effects or a special gold–support interface [1].

The reactivity of the monoclinic ZrO₂ support used was also tested at 513 K. Under the conditions applied, the activity was clearly below the detection limit.

3.1.2. Gold particle size dependence

A suitable method for varying the gold particle size was suggested by Haruta [1]. In a deposition–precipitation route the gold particle size was controlled by varying the pH value during precipitation. This gave rise to a decrease of mean gold particle size with increasing pH value. Indeed,

this method was successful for our objective. The gold particle size was examined by TEM imaging (as an example, see Fig. 1) and subsequent image analysis. While the size distribution of the sample Au/ZrO₂-DP24 precipitated at pH 9 fitted well to a logarithmic normal distribution, this was not observed for the others. Therefore, the mean particle size is generally calculated assuming a Gauss distribution to get comparable values. Moreover, since the catalytic properties are linked with the surface of the catalysts, the surface-averaged mean particle diameters were used. From the latter, the degree of dispersion D was estimated, enabling the calculation of a TOF. This was an important step, since the standard tool for dispersion measurement, hydrogen chemisorption, is not accessible for gold [21]. For our series of samples the mean particle size decreases with increasing pH value, as expected (Table 1, Fig. 2).

The catalytic experiments under identical conditions revealed a decrease of the TOF with particle size in the range from 4 to 8 nm. The maximum selectivity to allyl alcohol (44%) was achieved on Au/ZrO₂-DP22 at a temperature of 593 K (conversion 18%). Since at this temperature the gold-free ZrO₂ is not inert anymore (conversion 1%), all further

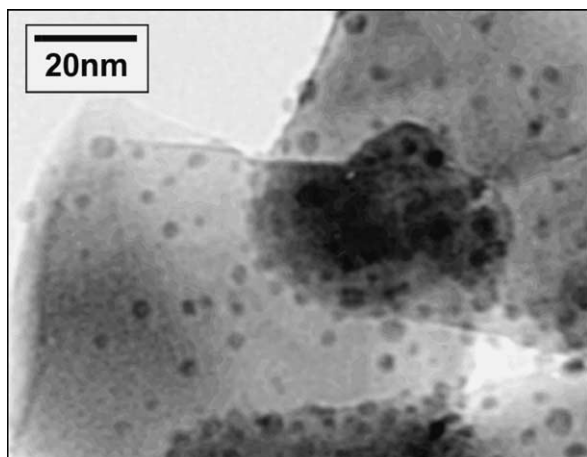


Fig. 1. TEM image of the sample Au/ZrO₂-DP24.

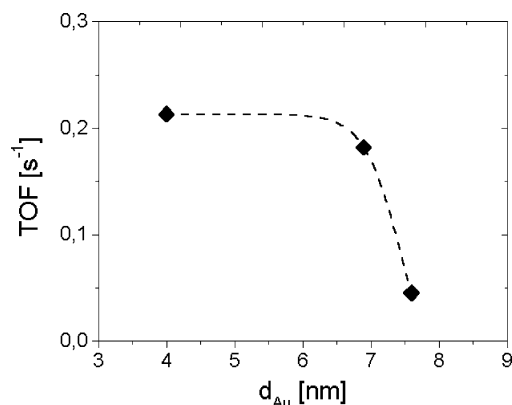


Fig. 2. Dependence of TOF from mean gold particle size d_{Au} at 513 K. From right to left: samples Au/ZrO₂-DP22, Au/ZrO₂-DP23, and Au/ZrO₂-DP24.

measurements were performed at 513 K to eliminate this influence. At this temperature, there is a distinct increase in selectivity to allyl alcohol with increasing particle size under identical conditions (Table 1; compare catalysts Au/ZrO₂-DP22, Au/ZrO₂-DP23, and Au/ZrO₂-DP24, each reduced at 573 K), accompanied by a decreasing selectivity of *n*-propanol and C₂ and C₃ hydrocarbons. To exclude the dependence of selectivities on the level of activity, two samples with the smallest and largest mean particle size, respectively, were chosen (Au/ZrO₂-DP24 and Au/ZrO₂-DP22). For Au/ZrO₂-DP24, the reciprocal space time $W/F_{Ac,0}$ was varied in such a way that a comparison of selectivities was possible with almost the same acrolein conversion (5%). This was the case for $W/F_{Ac,0} = 6.8 \text{ g h mol}^{-1}$ (Table 1). Under these experimental conditions again a increase of selectivity to allyl alcohol with increasing gold particle size was observed.

These experiments could support previously suggested models of different authors [10,15,16] for the dependence of the catalytic properties of metallic nanoparticles on their size. Namely, particles of cuboctahedral shape exhibit with increasing size an increasing amount of surface atoms residing on faces as compared to atoms in edges and corners [14]. Since ZrO₂ is a support of low interaction, this would imply that face atoms, most probably atoms in (111) surfaces, promote preferentially the hydrogenation of the C=O bond to get allyl alcohol [10]. To prove the validity of this structural model, a HRTEM examination was carried out to elucidate the real crystal structures of the gold particles.

3.2. Real structure of gold particles and catalysis

3.2.1. Validity of particle shape models

From thermodynamic considerations, by applying the so-called Wulff plot, the equilibrium shape of gold particles is derived. The actual particle shape depends on the differences of surface energies for different crystal faces. With the fcc metal gold, this geometrical model is a cuboctahedron (at 0 K). For increasing temperatures a transition to a rounded shape occurs [24]. This results in the occurrence of new crystal faces (for example, (311), (110)) as well as the decrease of the relative amount of (111) or (100) faces [25]. Besides, as known for more than 40 years from electron microscopic observations, completely different particle shapes, based on five-fold symmetry, may exist in the size range of the supported gold particles in the study presented here [26]. Extended electron microscopy studies including image simulations by many authors revealed the structure and shape of such particles [27–29]. They are composed of tetrahedral subunits which are connected by twin defects. Distortions are necessary to compensate for the lack of space filling emerging in this construction. In contrast, gold cuboctahedra exhibit exclusively the face-centered cubic crystal structure of the bulk. Possible shapes of these so-called multiply twinned particles (MTPs) are icosahedra and decahedra, respectively. Ball models of possible particle

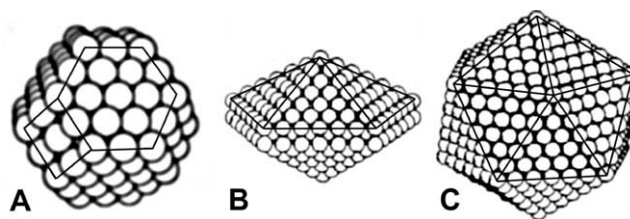


Fig. 3. Ball models of truncated cuboctahedron (A), decahedron (B), and icosahedron (C).

shapes are sketched in Fig. 3. For catalysis, the surface of the particles is of relevance, which is different in the case of MTPs, compared to fcc [30]. First of all, unusual surface sites may occur at the twin boundaries, since atoms may have hcp coordination rather than fcc. The relative number of atoms in such surface sites for a particle having a diameter of 10 nm is about 7%. Even though twins are also found in fcc particles, the surface of MTPs is characterized by a higher density of these twin boundaries.

Moreover, the relative number of (111) surfaces increases for MTPs, compared to a cuboctahedron of the same size. In the case of icosahedra, (100) faces completely disappear. The influence of the latter effect is reduced on rounded particles.

Additionally, MTPs exhibit elastic strain, which is on the order of magnitude of fluctuations of the lattice distance between different individual fcc particles [31,32]; strain effects should play only a minor role.

Particles of perfect single-crystal structure are assigned as SC, though there is partially a slight deviation from their perfect fcc structure. Such particles, exhibiting a single planar defect (single twin), are assigned to ST.

The different types of particle shapes can be assigned by comparing digitized HRTEM images of individual particles and their diffractograms, generated by Fourier transform, with models and images of known particle shapes in various possible orientations. A scheme of resulting patterns is shown in Fig. 4. Such assignments are justified by the vast number of image simulations of such structures (see, for example, [27–29]).

Up to now, there were only a very few studies concerned with the role of multiply twinned particles in the field of catalysis. Yacaman et al. [33] used electron microscopy (electron diffraction as well as image contrast simulations) for structural characterization of Rh particles on *M* (*M* = Al₂O₃, SiO₂, TiO₂, C) as catalysts for pentane hydrogenolysis. The identification of particle shapes was done by comparison with image contrast simulations. An unambiguous correlation between the occurrence of MTPs and catalytic activity was not found. Vogel et al. performed experiments on Au/TiO₂ [34] and Au/Mg(OH)₂ [35], used as catalysts in the oxidation of CO. They applied Debye functional analysis to identify the different particle shapes from X-ray diffraction. While for Au/TiO₂ single crystalline particles were found to be the dominating species, for Au/Mg(OH)₂ a distinct increase in activity was explained

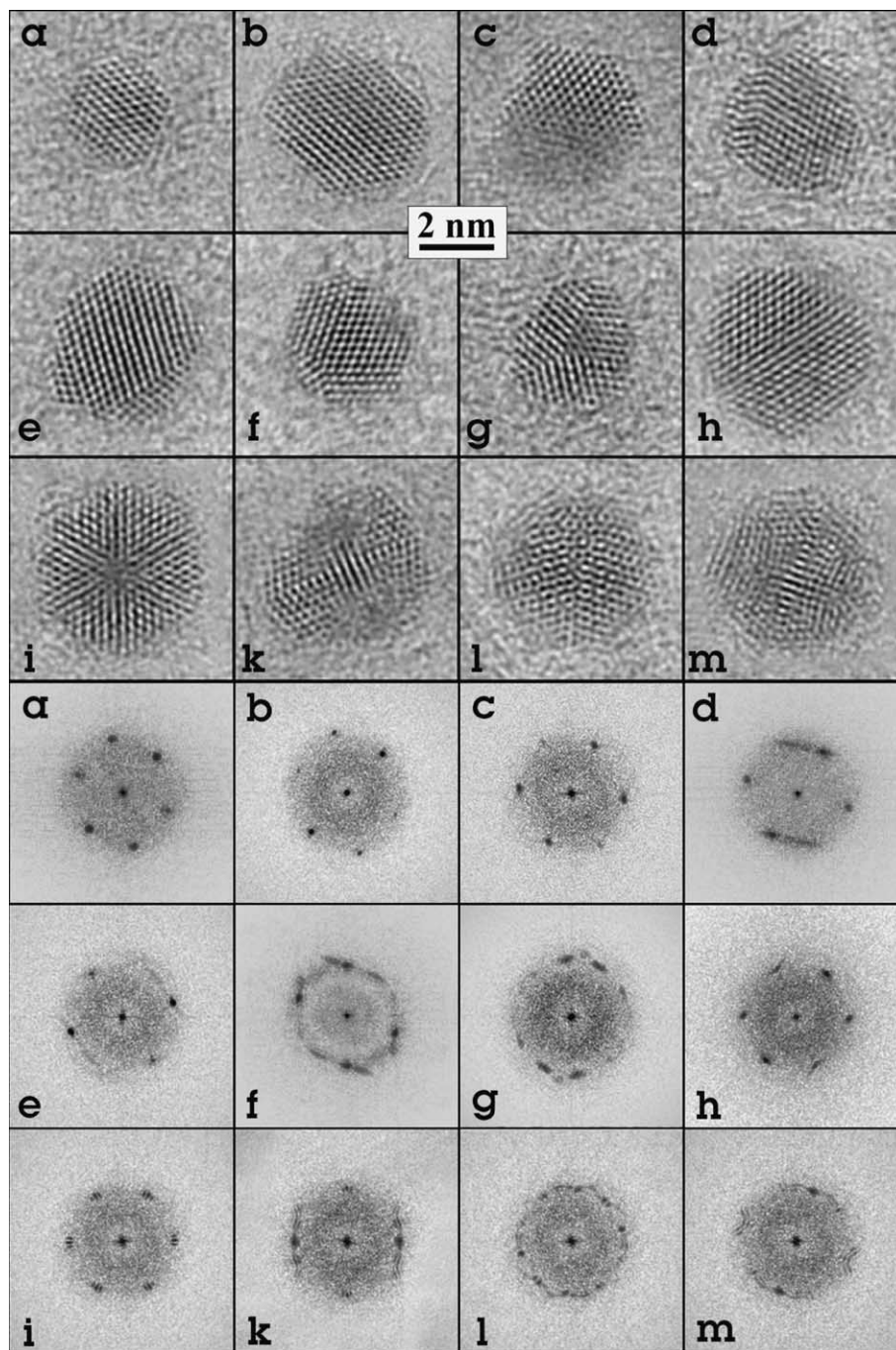


Fig. 4. Tableau for identification of particle structures in HRTEM, taken from Ag particles [10] (usage see text). Upper part: real-space images; lower part: corresponding calculated diffractograms. Assignment: a, b: single crystals (SC); c, d: single twins (ST); e–h: decahedra; i–m: icosahedra.

by the appearance of icosahedra. However, the influence of MTPs could not be separated clearly from additional influences of particle size and the degree of rounding.

To prove what kind of particle shapes occur in our samples, the two samples with the smallest and largest mean particle size (Au/ZrO₂-DP24 and Au/ZrO₂-DP22) were chosen again and statistics on the shape of individual particles were performed (Fig. 5). Beside single crystalline particles (SC) and MTPs, particles with a single planar

defect (ST) and very seldom particles showing a mixture of planar defects and MTP-like defects (sometimes termed “polyparticles”) were also found. Since the amount of the latter was distinctly below 5%, it was neglected in the figures for the sake of clarity.

The assignment to one of these categories may be ambiguous for a few particles showing not well established contrast, leading to confusion, most probably between SC and ST, ST and MTP, and icosahedra and decahedrons, re-

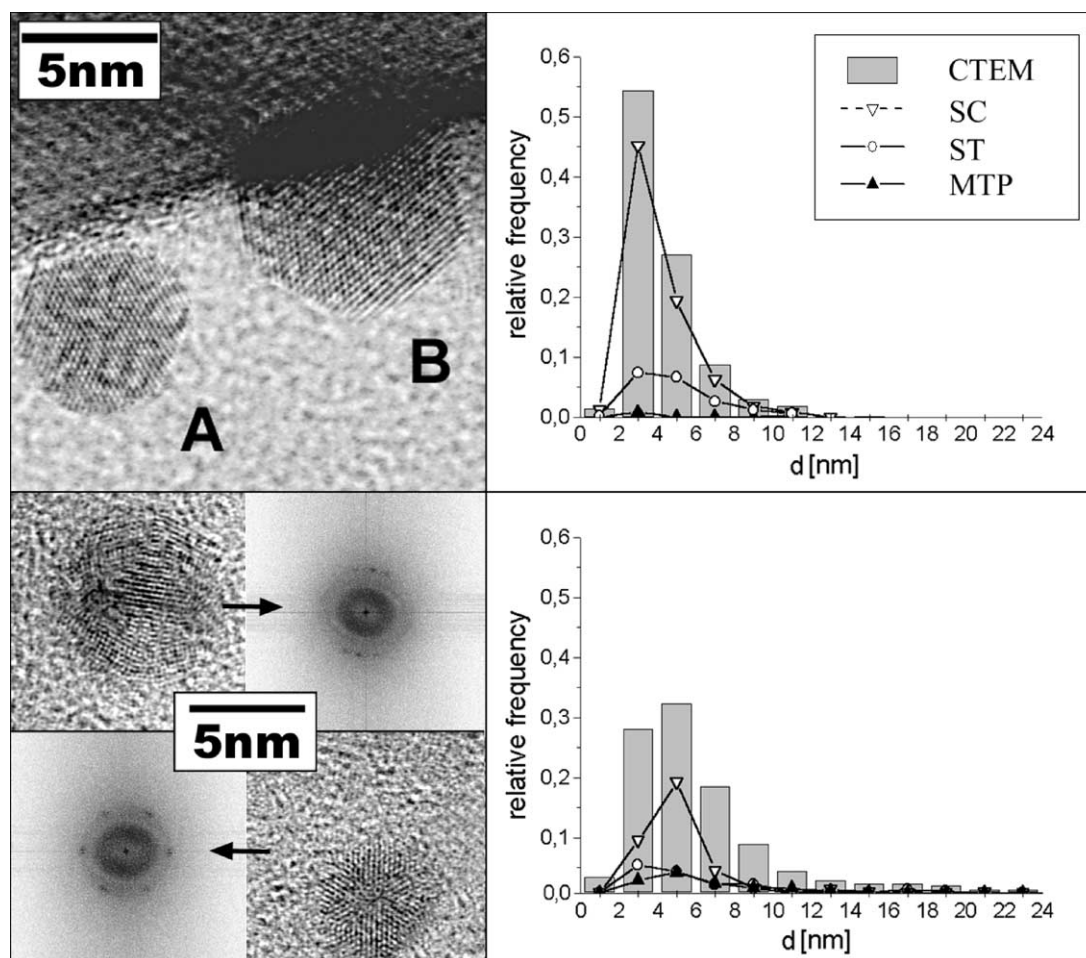


Fig. 5. Upper row (left): representative HRTEM image of sample Au/ZrO₂-DP24 with a more rounded gold particle (A) and a particle with facets (B). Upper row (right): separate size distributions of single crystalline gold particles (SC), single twinned particles (ST) and multiply twinned particles (MTP) together with overall size distribution measured by TEM. Lower row (left): HRTEM images of multiply twinned particles of sample Au/ZrO₂-DP22 and corresponding diffractograms. Lower row (right): gold particle size distributions.

spectively. In spite of these difficulties, the discrimination between SC and MTP was much more obvious. To make the evaluation representative despite relying on local measurements, a larger number of particles (about 400 to 500) were analyzed.

Indeed, significant differences between the different samples were found. Whereas in the sample Au/ZrO₂-DP24 most of the particles have SC or ST shape (Fig. 5, upper row), in the sample Au/ZrO₂-DP22 there was a significantly increasing portion of MTPs (Fig. 5, lower row).

The main part (~70–80%) of them are icosahedra. Since the summation of decahedra and icosahedra did not influence the interpretation of the catalytic behavior, we did not further distinguish between the two species of MTPs. Thus, the final task, namely the discrimination between SC and MTP under consideration of ST, was easily achieved with our method, regardless of the above-mentioned restrictions.

Moreover, in both samples faceted particles as well as more rounded particles were found, but the relative number of facets was slightly higher for sample Au/ZrO₂-DP22.

The structure sensitivity, i.e., the particle size dependence of activity and selectivities, is assumed to be a cooperative effect of particle size, degree of rounding, and portion of MTPs. A correlation of the HRTEM analysis with catalytic results reveals that a cuboctahedral single crystal model is not in general applicable as a model for gold particles. Thus, a simple deduction of the nature of active sites based on the cuboctahedral model of van Hardefeld and Hartog [14] is not possible.

3.2.2. Influence of MTPs on catalysis

To clear up the impact of MTPs on reactivity in the hydrogenation of acrolein, the proportions of such icosahedra and decahedra were systematically varied, according to suggestions of Doraiswamy and Marks [36]. Therefore, time and temperature of reduction in flowing hydrogen were varied separately (Table 1). Increasing the time of the reduction from 3 to 18 hours at 573 K increases not only the amount of MTPs by a factor of 2, but furthermore also the mean particle size from 7.6 to 9.2 nm if one compares the surface-averaged mean diameter values (Fig. 6). By increasing the tempera-

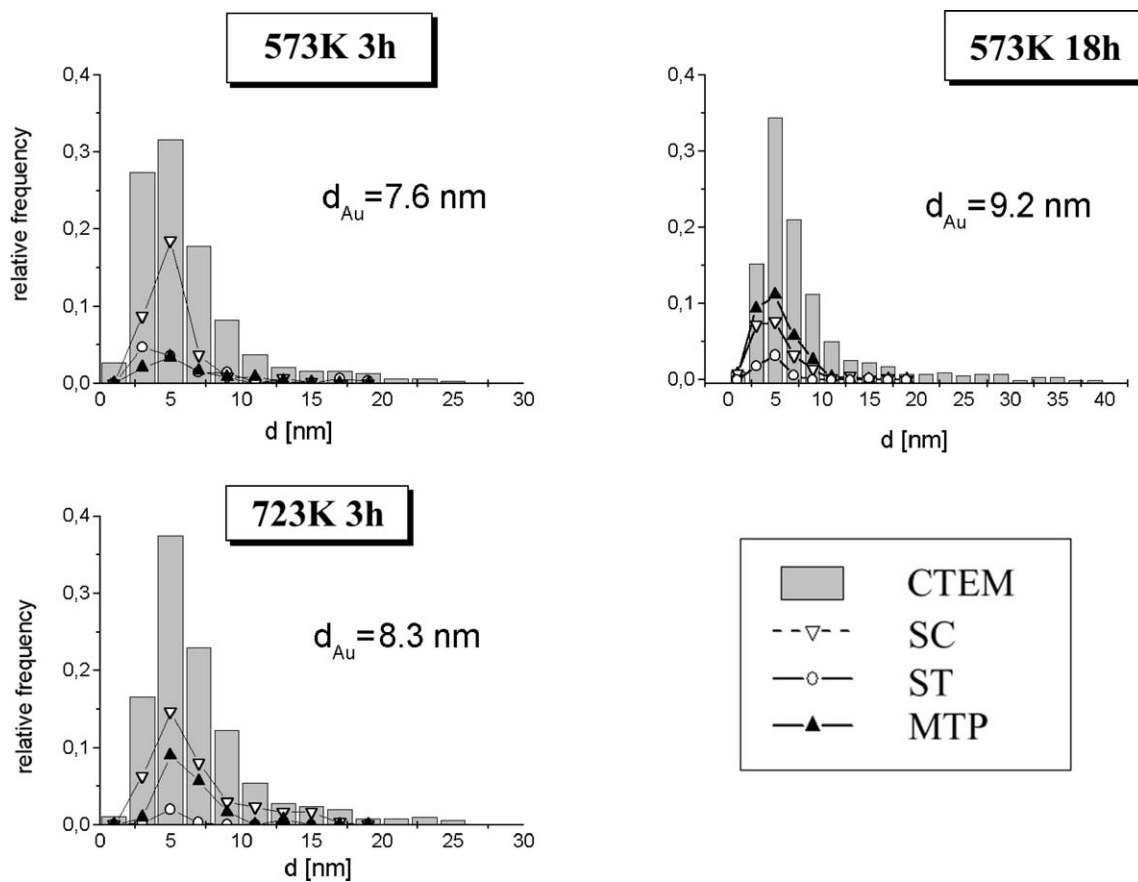


Fig. 6. Separate size distributions of single crystalline gold particles (SC), single twinned particles (ST), and multiply twinned particles (MTP), together with overall size distribution measured by TEM of the different samples based on Au/ZrO₂-DP22, prepared under different conditions of pretreatment in hydrogen.

ture of reduction from 573 to 723 K, the relative amount of MTPs does not change measurably, and the mean particle diameter increases again, but weaker. In all of these samples the gold particles were to a certain extent rounded. Hence, an additional influence of different degrees of rounding can be excluded. Simultaneously, the catalytic activities and selectivities were recorded. Besides the desired allyl alcohol, only propionaldehyde was detected as a product of the consecutive C=C hydrogenation. All other products possible, in principle, were found only in trace amounts. This allows the direct comparison of selectivities also for different TOF:

1. Increasing the reduction time from 3 to 18 h leads to a drop in selectivity to the desired allyl alcohol as well as to a decrease of TOF.
2. Increasing the reduction temperature from 573 to 723 K does not change the TOF and just slightly increases the selectivity to allyl alcohol.

There are some obvious correlations between particle shape and catalytic properties. A decrease of TOF and allyl alcohol selectivity after an increase of the reduction time from 3 to 18 h is accompanied by an increase of the relative number of MTPs and an increase of mean particle

size. The influence of the latter can be ruled out since an increase of the reduction temperature from 573 to 723 K led also to an increase of mean particle size, but did not decrease TOF and allyl alcohol selectivity (see Table 1). Furthermore, an additional influence of faceting effects is low, since the gold particles are generally slightly rounded, independent on the hydrogen treatment conditions. Thus, the only parameter responsible for the drop in selectivity is the increasing portion of MTPs.

3.2.3. Influence of degree of rounding

Different degrees of rounding of metal particles may be realized to a certain extent by changing the pretreatment temperature, if the value of the latter is not too high [37]. However, it is almost impossible to realize in this way different degrees of rounding without changing the mean particle size or the proportion of MTPs.

Another factor influencing the degree of rounding may be the kind of support, due to different metal support interactions. To evaluate such a support effect, a reference catalyst supported on TiO₂ is used, which has been investigated recently by us [12]. This sample was produced by a deposition–precipitation procedure as well and is designated as Au/TiO₂-DP. A typical HRTEM image is shown in

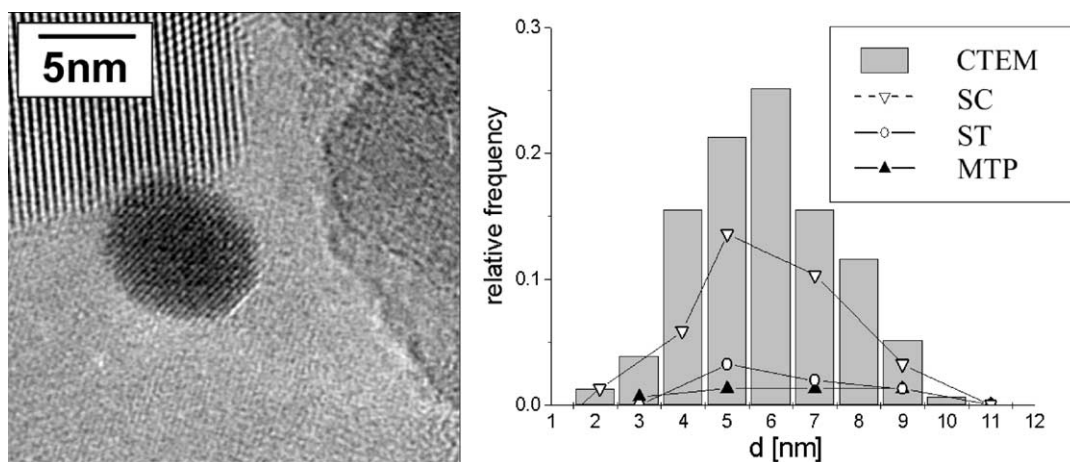


Fig. 7. (Left) HRTEM image of Au/TiO₂-DP showing the occurrence of rounded gold particles. (Right) separate size distributions of single crystalline gold particles (SC), single twinned particles (ST), and multiply twinned particles (MTP) together with overall size distribution measured by TEM [12].

Fig. 7, together with separate size distributions of the gold particles exhibiting different shapes. It is obvious that the gold particles are not faceted at all, and furthermore the contribution of MTPs can be neglected. The mean gold particle size is $d_{\text{Au}} = (5.3 \pm 0.3)$ nm [12]. Thus it may be possible to compare this catalyst with Au/ZrO₂-DP22, since the latter has also a negligible amount of MTPs and a similar particle size. The results of acrolein hydrogenation are shown in Fig. 8. It is clearly seen that the TOF of the titania-based catalyst is higher by a factor of about 2. A comparison of the allyl alcohol selectivities is complicated, since an additional dependence of the selectivities on the activity itself must be taken into account. This results in nonnegligible selectivities of *n*-propanol and C₂ and C₃ hydrocarbons.

The increase of TOF for Au/TiO₂ may be well explained by more rounded gold particles, accompanied by a higher relative amount of low-coordinated surface sites. Increasing activities on such surface sites were indeed found for other systems (CO oxidation on supported Au particles [39]).

Besides, in the case of titania-based gold catalysts, the generation of active sites on the interface between gold support is often suggested [1,7,38]. Such an additional effect cannot be completely ruled out. Further metal–support

interactions could be due to electron transfers. However, for Au/TiO₂ catalysts this is unlikely [39,40].

The catalytic measurements on gold powder support the assumption of sole participation of the gold surface in the hydrogenation process: Even though the calculated TOF of the gold powder is not directly comparable with that of the supported gold catalysts, since there is a difference in the residence times (see Table 1), the range of activities is roughly the same. Even though additional influences (as explained above) cannot be excluded by this experiment, this result is a strong indication of a major contribution of the gold surface itself to the catalytic process.

4. Conclusions

Hydrogenation of acrolein works under the conditions used even on bulk-like gold powder, although the selectivities to the desired product, allyl alcohol, are much lower than for gold nanoparticles on supports. Thus the activation process on gold is neither exclusively limited to quantum size effects nor induced by the supports or a special design of the gold–support interface, as assumed for oxidation reactions on gold [1]. A higher selectivity to the desired allyl

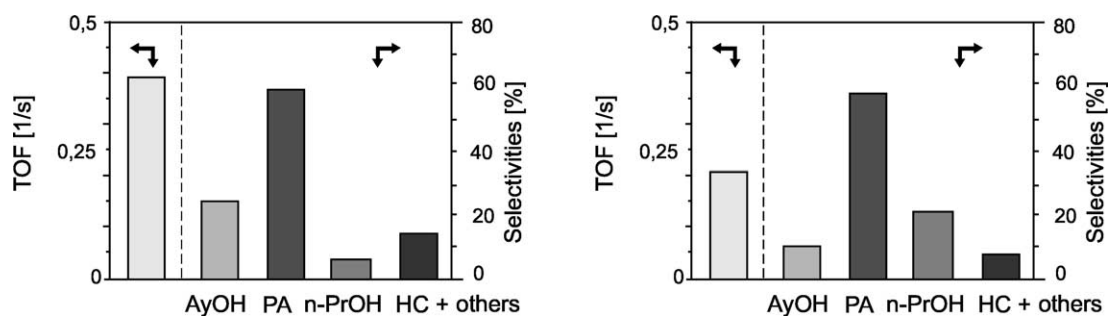


Fig. 8. Comparison of Au/TiO₂-DP (left) [12] and Au/ZrO₂-DP24 (right) in hydrogenation of acrolein at 513 K.

alcohol seems to be restricted to smaller gold particles, i.e., to special surface sites accessible to a large extent only on these particles.

The selective hydrogenation of acrolein is a structure-sensitive reaction on Au/ZrO₂ catalysts. The TOF increases with decreasing particle size, while the allyl alcohol selectivity decreases in that direction. This may be a result of superposition of different effects, i.e., due to a changing proportion of different sites on the gold surface (particle size effect—different proportions of edges, faces, etc.—or rounding effect) and differing numbers of MTPs. Therewith, the sole application of a cuboctahedral model to describe the structure sensitivity is not useful.

Furthermore, the first systematic study on the influence of the real structure of the active metallic component on activity and selectivity in the hydrogenation of α , β -unsaturated aldehydes was performed. The influence of particle shape has been studied independent of particle size effects or rounding effects. It has been shown that an increasing number of MTPs leads to a decrease in TOF and allyl alcohol selectivity. The low applicability of MTPs may principally have different reasons. Since the gold particles are in general rounded, the catalytic effect should be due only to a minor part to an elevated relative number of (111) surfaces for MTPs. Hence, a more probable explanation includes the effect of higher density of twin boundaries. The higher TOF of a Au/TiO₂ catalyst compared to Au/ZrO₂ has been ascribed to the higher degree of rounding of the dominating single crystalline fcc particles, i.e., a higher portion of low-coordinated surface sites.

Acknowledgments

This work has been supported by the Federal Ministry for Science and Education under Grant 03D0028A0. P.C. thanks the Fonds der Chemischen Industrie for financial support. C.M. and P.C. are grateful to I. Dambowski and R. Eckelt (Institute for Applied Chemistry, Berlin) for ICP-OES analyses and for the preparation of the gold powder, respectively.

References

- [1] M. Haruta, *Catal. Today* 36 (1997) 153.
- [2] G.C. Bond, P. Sermon, G. Webb, D.A. Buchanan, P.B. Wells, *J. Chem. Soc. Chem. Commun.* (1973) 444.
- [3] G.C. Bond, P.A. Sermon, *Gold Bull.* 6 (1973) 102.
- [4] P.A. Sermon, G.C. Bond, P. Wells, *J. Chem. Soc. Faraday Trans.* 75 (1979) 385.
- [5] M. Shibata, N. Kawata, T. Masumoto, H. Kimura, *J. Chem. Soc. Chem. Commun.* (1988) 154.
- [6] J. Jia, K. Haraki, J.N. Kondo, K. Domen, K. Tamaru, *J. Phys. Chem. B* 104 (2000) 11153.
- [7] J.E. Bailie, J.G. Hutchings, *J. Chem. Soc. Chem. Commun.* (1999) 2151.
- [8] J.E. Bailie, H.A. Abdullah, J.A. Anderson, C.H. Rochester, N.V. Richardson, N. Hodge, J.-G. Zhang, A. Burrows, Ch.J. Kiely, G.J. Hutchings, *Phys. Chem. Chem. Phys.* 3 (2001) 4113.
- [9] J.E. Bailie, G.J. Hutchings, *Catal. Commun.* 2 (2001) 291.
- [10] P. Claus, H. Hofmeister, *J. Phys. Chem. B* 103 (14) (1999) 2766.
- [11] C. Mohr, H. Hofmeister, M. Lucas, P. Claus, *Chem. Eng. Technol.* 3 (4) (2000) 324.
- [12] P. Claus, A. Brueckner, C. Mohr, H. Hofmeister, *J. Am. Chem. Soc.* 122 (46) (2000) 11430.
- [13] M. Che, C. Bennett, *Adv. Catal.* 36 (1989) 55.
- [14] R. van Hardefeld, F. Hartog, *Surf. Sci.* 15 (2) (1969) 189.
- [15] M. Englisch, A. Jentys, J.A. Lercher, *J. Catal.* 166 (1) (1997) 25.
- [16] A. Giroir-Fendler, D. Richard, P. Gallezot, *Catal. Lett.* 5 (2) (1990) 175.
- [17] Scion Image, available at: <http://www.scioncorp.com>.
- [18] M. Lucas, P. Claus, *Chem.-Ing.-Technol.* 67 (1995) 773.
- [19] J.R. Anderson, in: *Structure of Metallic Catalysts*, Academic Press, London, 1975, p. 360.
- [20] J.M. Montejano-Carrizales, F. Aguilera-Granja, J.L. Moran-Lopez, *NanoStructured Mater.* 8 (3) (1997) 269.
- [21] G.C. Bond, D.T. Thompson, *Catal. Rev. Sci. Eng.* 41 (3–4) (1999) 319.
- [22] P. Gallezot, D. Richard, *Catal. Rev. Sci. Eng.* 40 (1–2) (1998) 81.
- [23] P. Claus, *Fine Chemicals Catalysis* 5 (II) (1998) 51, Special Issue.
- [24] C.R. Henry, *Surf. Sci. Rep.* 31 (1998) 235.
- [25] E.G. Schlosser, *Ber. Bunsenges. Phys. Chem.* 73 (8–9) (1969) 929.
- [26] H. Hofmeister, *Cryst. Res. Technol.* 33 (1998) 3.
- [27] P.A. Buffat, M. Flueli, R. Spycher, P. Stadelmann, J.P. Borel, *Faraday Discuss.* 92 (1991) 173.
- [28] C.Y. Yang, M.J. Yacaman, K. Heinemann, *J. Cryst. Growth* 47 (2) (1979) 283.
- [29] C.Y. Yang, *J. Cryst. Growth* 47 (2) (1979) 274.
- [30] L.D. Howie, A. Marks, *Nature* 282 (1979) 196.
- [31] K. Koga, H. Takeo, T.O.K. Ikeda, *Phys. Rev. B* 57 (7) (1998) 4053.
- [32] C. Mohr, H. Hofmeister, M. Dubiel, *J. Phys. Condens. Matter* 13 (2001) 525.
- [33] M.J. Yacaman, S. Fuentes, J.M. Dominguez, *Surf. Sci.* 106 (1981) 472.
- [34] D.A.H. Cunningham, W. Vogel, R.M.T. Sanchez, K. Tanaka, M. Haruta, *J. Catal.* 183 (1999) 24.
- [35] (a) W. Vogel, D.A.H. Cunningham, K. Tanaka, M. Haruta, *Catal. Lett.* 40 (3–4) (1996) 175;
(b) D.A.H. Cunningham, W. Vogel, H. Kageyama, S. Tsubota, M. Haruta, *J. Catal.* 177 (1998) 1.
- [36] N. Doraiswamy, L.D. Marks, *Philos. Mag. B* 71 (3) (1995) 291.
- [37] F. Cosandey, T.E. Madey, *Surf. Rev. Lett.* 8 (1–2) (2001) 73.
- [38] C. Mohr, P. Claus, *Sci. Progr.* 84 (4) (2001) 311.
- [39] S. Schimpf, M. Lucas, C. Mohr, U. Rodemerck, A. Brueckner, J. Radnik, H. Hofmeister, P. Claus, *Catal. Today* 72 (2002) 63.
- [40] A. Goossens, M.W.J. Crajé, A.M. van der Kraan, A. Zwijnenburg, M. Makkee, J.A. Moulijn, L.J. de Jongh, *Catal. Today* 72 (2002) 95.